32nd European Modeling & Simulation Symposium
17th International Multidisciplinary Modeling & Simulation Multiconference

ISSN 2724-0029 ISBN 978-88-85741-44-7 © 2020 The Authors.
DOI: 10.46354/i3m.2020.emss.051

Silicon nitride focusing grating coupler for input and output light of NV-centers

Aleksei Kuzin[1,2,*], Ilia Elmanov[2], Vadim Kovalyuk[2], Pavel An[2] and Gregory Goltsman[2,3]

[1]Skolkovo Institute of Science and Technology, 121205, Russia
[2]Department of Physics, Moscow State Pedagogical University, 119992, Russia
[3]National Research University Higher School of Economics, Moscow, 101000, Russia

*Corresponding author. Email address: Aleksei.Kuzin@skoltech.ru

Abstract

Here we presented the numerical results for the calculation of focusing grating coupler efficiency in the visible wavelength range. Using the finite element method, the optimal geometric parameters, including filling factor and grating period for a central wavelength of 637 nm, were found. Obtained results allow to input/output single-photon radiation from NV-centers, and can be used for research and development of a scalable on-chip quantum optical computing.

Keywords: Photonic integrated circuits (PICs), Focusing grating coupler (FGC), NV-centers in diamond

1. Introduction

A photonic integrated circuit (PIC) based on silicon nitride (SiN) film is one of the most promising platforms for on-chip quantum photonics (O'Brien et al., 2009). This is due to both the ability to work in the visible and near-infrared wavelengths with low optical losses and CMOS fabrication capabilities. Integration and research of single-photon sources for the needs of on-chip linear optical quantum computing (LOQQ) remain one of the main tasks for scalable processing. If at the final stage of implementing such schemes, photons will be generated and detected on-chip, without coupling outside, at this moment, the development of efficient light couplers from NV-centers atop of waveguide is needed.

Here, we numerically investigated a focusing grating coupler (FGC) design for one of the most studied solid-state quantum emitter (NV-center in diamond) close to its zero-phonon line wavelength (637 nm).

FGCs for visible wavelength range were demonstrated earlier (Song et al., 2019), but suffered from significant coupling losses or complex technological fabrication and should be optimized further.

In this paper, 2D modeling of the focusing grating coupler for NV-centers radiation was performed. The optimal waveguide width for single-mode light propagation and the dependence of losses on the thickness of silicon oxide were found. The dependences of the grating period on the filling factor providing the central wavelength of 637 nm, as well as color contour map of the efficiency were studied. Based on the data obtained, ways for further development for this study were selected.

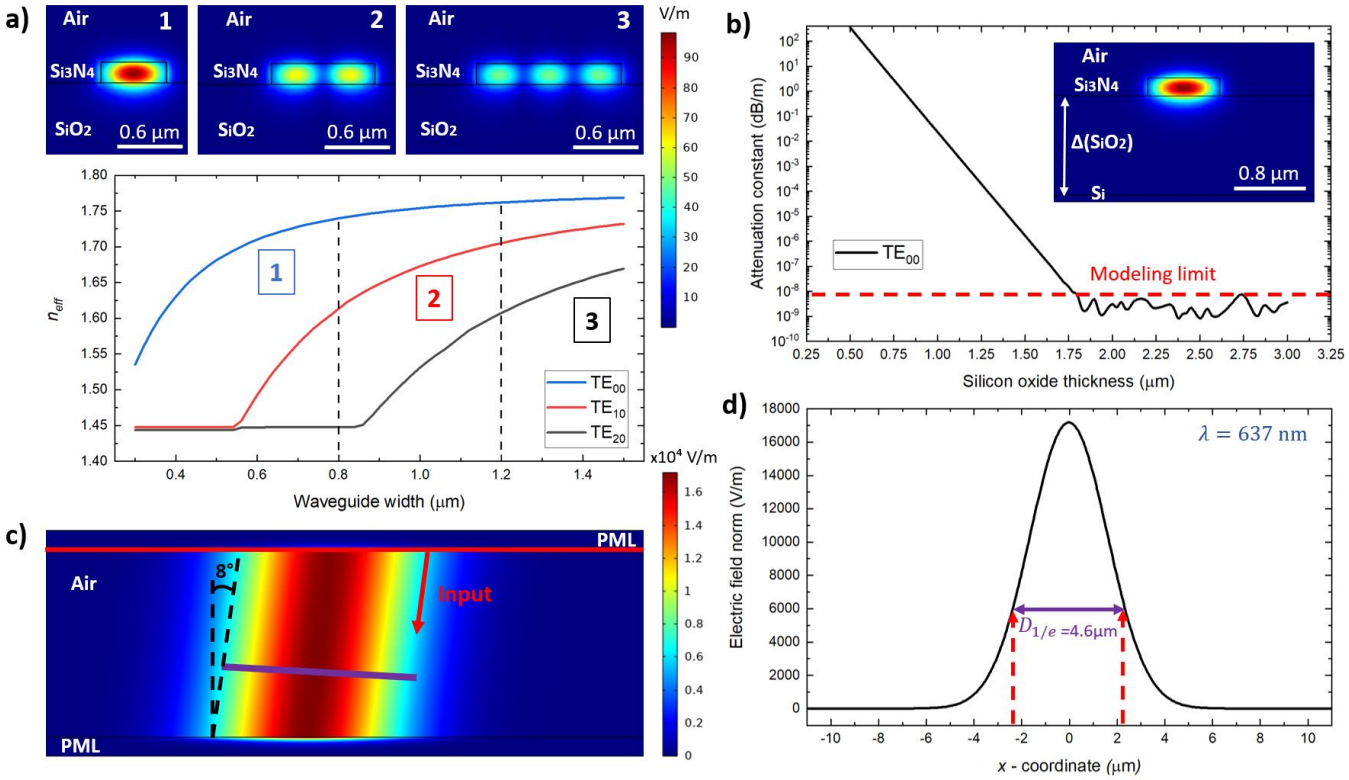

Figure 1. a) Dependence of the effective refractive index on the waveguide width for TE modes. The blue, red and black lines show the fundamental, second and third TE modes, respectively. The dashed lines indicate the regions, where the transition between modes occurs. The upper part of the figure shows the normalized electric field distribution depending on the width of the waveguide. **b)** Dependence of the attenuation constant on the SiO_2 thickness for the fundamental TE mode. The insert shows a variable parameter of SiO_2 thickness, tuned during calculations. The red dotted line shows the accuracy of the model, associated with the minimum size of finite elements. **c)** Distribution of normalized electric field when Gaussian beam at λ = 637 nm incidents at an angle of 8 degrees. The perfect match layer (PML) covers all the entire boundaries. **d)** Dependence of the normalized electric field on the coordinate for a Gaussian beam. The Gaussian beam falls at an angle of 8 degrees to the normal. The mode field diameter is equal to 4.6 µm at a wavelength of 637 nm.

2. State of the art

Currently, many interesting works to improve the coupling efficiency of the FGCs have been done (Cheng et al., 2020).

Some of the articles demonstrated an increase in the FGC efficiency using the bottom distributed Bragg reflectors. The authors presented high-performance gratings for the silicon nitride platform (Nambiar et. al., 2019). The coupling efficiency for the best device was -2.29 dB per coupler. Using the bottom Bragg reflector, the highest efficiency for the silicon nitride film thickness in a range of 400 and 500 nm at the telecommunication wavelength of 1.55 µm were demonstrated. Other researchers optimized geometric parameters of FGCs, such as taper angle or taper length (Kuzin et al., 2019), or changing the device design (Hoffmann et al., 2018). However, most of the works considered the telecommunication wavelength range.

In the visible wavelength range, using a numerical FDTD (Finite Difference Time Domain) method, an elliptical FGC with the additional metal layer to improve the coupling efficiency was designed (Wang, et. al., 2012). The authors obtained high efficient FGC and a narrow radiation pattern, using a similar concept for the visible light instead of infrared (IR) range. The article also notes that the fabrication of couplers with a partial etching can be quite difficult, due to variation of the etching depth. However, the grating coupler was optimized near our interest at around 632.8 nm and was used as a starting point.

3. Materials and Methods

Modeling of FGC for NV-center radiation was performed using the finite element method (FEM) implemented in COMSOL Multiphysics. As a material for a numerical model, we used commercially available wafers with 200 nm thick silicon nitride film atop of silicon substrate with 2µm SiO_2 spacer. The real and imaginary parts of the refractive index versus the wavelength were specified in the model. The minimum mesh size was determined as 40 nm. The Numeric port type was used for input and output light.

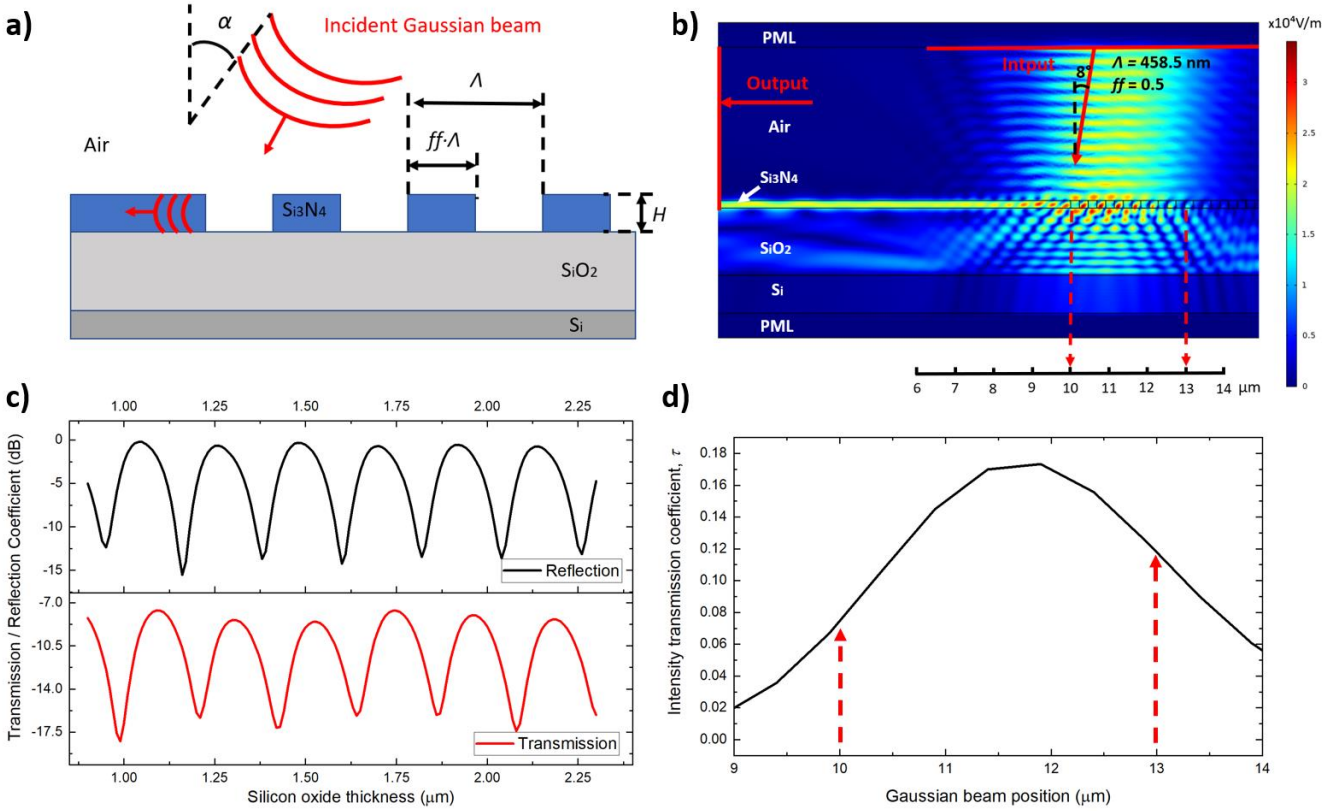

Figure 2. a) Schematic view of a FGC and the Gaussian beam incident at an angle of 8 degrees to the grating normal. α – angle of incidence for the Gaussian beam. *ff* is filling factor, Λ is grating period, H is Si_3N_4 thickness. **b)** Normalized electric field for Gaussian beam incident at 8 degrees to the normal of the FGC. The grating period is 470 nm, the filling factor is 0.5. **c)** Transmittance and reflection coefficients versus silicon oxide thickness for the following grating parameters: *ff* = 0.5, Λ = 470 nm, H = 200 nm. **d)** Dependence of the simulation data for intensity transmission coefficient τ on the Gaussian beam position.

To decrease undesirable reflections, perfect match layers (PML) covered all boundaries inside the model. The incident beam had the Gaussian beam profile and propagated at an angle of 8° to the FGC normal. The diffraction of the FGC was specified using the phase matching condition (the Bragg condition):

$$mG + k_0 sin\theta = 2\beta_m, \quad (1)$$

where G is the grating vector and m is the grating diffraction order (Cheng et al., 2020). This condition is used to set the relationship between the wave vector k_o of the incident light beam and the propagation constant β. The intensity transmission coefficient τ was specified as an absolute value of S_{21} parameter (transmission) squared according to the Fresnel formulas.

4. Results and Discussion

At the first stage of the study, we selected the geometrical parameters of the Si_3N_4 waveguide to ensure a single-mode propagation condition inside. The 2D model of the waveguide cross-section for a waveguide width tuning is shown in Fig.1a. After a cut-off condition for waveguide width less than 400 nm and single-mode light propagation (TE_{00}), an increase in the waveguide width leads to the appearance of additional TE modes: TE_{10} and TE_{20}. The range of single-mode propagation up to 800 nm, and for the propagation of TE_{00} and TE_{10} simultaneously up to 1200 nm the waveguide width, highlighted by black dotted lines, is shown in Fig.1a.

In the second step, a numerical calculation of the optimal SiO_2 thickness was made. For this reason, a 70 nm Si layer with an imaginary and a real part of the refractive index was added into the waveguide cross-sectional model below SiO_2 (Fig.1b). By varying the thickness of silicon oxide $\Delta(SiO_2)$, the dependence of the fundamental TE_{00} optical losses was found. Fig.1b shows that optical losses can be neglected, starting from an oxide thickness of 1.5 μm (1dB per 1000 km).

In the third step, the optimal parameters for the Gaussian beam profile, according to standard equations (Alda, 2003) were found.

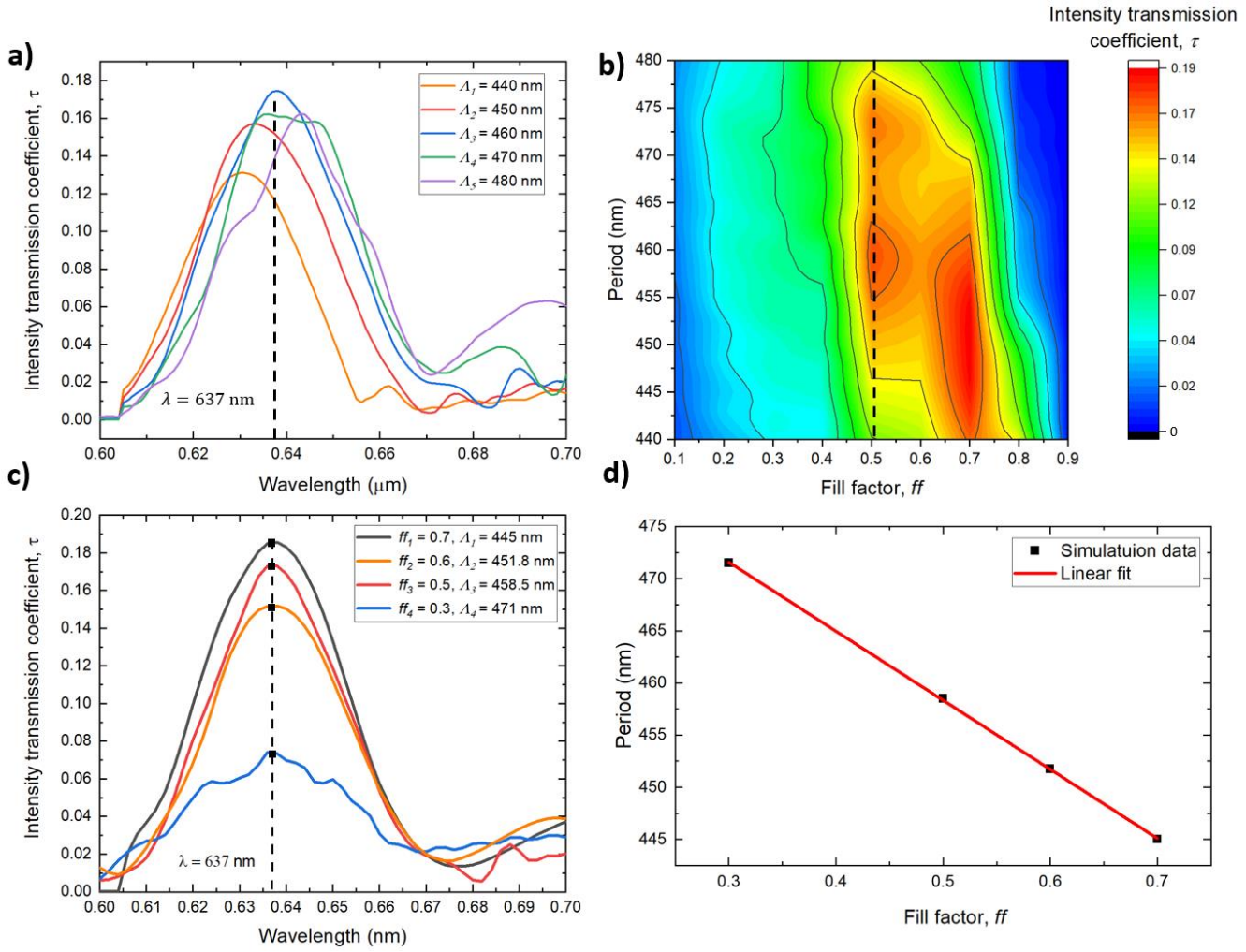

Figure 3. a) Intensity transmission coefficient versus wavelength for different periods at a fixed filling factor *ff* = 0.5. **b)** Color contour map of the coupling efficiency for 637 nm wavelength depending on filling factor and grating period. **c)** The dependence of the intensity transmission coefficient on the wavelength for different *ff* and *Λ*. Black dots denote the coupling efficiency for a wavelength of 637 nm at a fixed grating *ff* = 0.5. **c)** Dependence of the grating period on the filling factor providing the center wavelength of 637 nm.

Figure 1c shows the result of 2D simulation for a Gaussian beam incident at an angle of 8 degrees to the FGC normal at a wavelength of 637 nm. Here the Gaussian beam propagated in the air without the FGC. The perfect matched layer (PML) was used to decrease the reflection from all boundaries. Figure 1d shows the dependence of the normalized electric field distribution versus the Gaussian beam coordinate. For the further simulation, we used the mode field diameter equals to 4.6 μm, matched the commercially available single-mode fiber S405-XP.

In the fourth step, we used the generated Gaussian beam together with a longitudinal section of the FGC. Figure 2a shows a schematic view of the longitudinal section of the FGC, which indicates the main geometric parameters of the grating: filling factor (*ff*), period (*Λ*), the height of the Si_3N_4 layer (*H*). In Figure 2b the normalized electric field distribution for a side view of FGC is shown. In addition to phase-matched scattering by the grating, reflection at Si/SiO_2 interface, acting as a cavity, increased the overall coupling efficiency. To maximize the intensity transmission coefficient, the dependence of efficiency on the Gaussian beam position was calculated (Figure 2d). It was found the maximum efficiency of 19% at a distance of 1.5 μm from the waveguide taper. Such a distance corresponds approximately the region of the third grating tooth and was used for further calculations.

In the fifth step, the dependence of the intensity transmission coefficient on the SiO_2 thickness was obtained (Figure 2c). Taking into account the results associated with optical losses (Fig. 1c), the value of 1.75 μm as the optimal S_iO_2 thickness was chosen.

In the sixth step, we investigated the coupling efficiency of FGC at 637 nm wavelength as a function of filling factor and period. In Fig.3a shown the spectral coupling efficiency at the fixed filling factor of

0.5 and different periods. By doing similar calculations for various filling factors in a range of 0.1-0.9, we combined the obtained data and plotted the color contour map of the coupling efficiency depending on periods and fill factors simultaneously (Fig. 3b). The maximum efficiency is clearly seen near the filling factor of 0.7 and the period of 445 nm.

At the seventh step of the study, we found the parameters of the period and filling factor providing the center wavelength of 637 nm. The parameters were adjusted to maximize efficiency for a given wavelength (Figure 3c). Using these parameters, it was found between them a linear relationship (Figure 3d).

Based on the data obtained, it was found the maximum coupling efficiency of 19%, at a wavelength of 637 nm, at a filling factor of 0.7, a grating period of 445 nm, and Si_2O oxide thickness of 1.75 μm.

5. Conclusions

Using the finite element method (FEM), the optimal geometric parameters for a 2D grating coupler were found. To obtain the maximum efficiency at the central wavelength of 637 nm we varied beam position relative to the grating, as well as swept oxide thickness, FGC period and filling factor. The obtained data can be used both to study NV-centers apart (Aharonovich et al., 2016), as well as for fabrication scalable on-chip fully integrated quantum photonic circuits with single-photon sources, detectors, passive and active elements.

Further research is related to the study of the 3D model and the period-filling factor FGC apodization for the visible wavelength range.

Funding

The research was performed by support of Ministry of Education and Science of the Russian Federation (contract № 14.586.21.0063, unique identificatory RFMEFI58618X0063).

References

Aharonovich, I., Englund, D. and Toth, M. (2016). Solid-state single-photon emitters *Nat. Photon.*, 10:631-641.

Alda, J., Laser and Gaussian Beam Propagation and Transformation. *Encyclopedia of Optical Engineering.*

Cheng, L., Mao, S., Li, Zi., Han, Y. and Fu H. Y. (2020). Grating Couplers on Silicon Photonics: Design Principles, Emerging Trends and Practical Issues, *Micromachines*, 11, 666.

Hoffmann, J. et al. (2018). Backscattering design for a focusing grating coupler with fully etched slots for transverse magnetic modes. *Scientific Rep.*, vol. 8, 17746.

Kuzin, A. et al. (2019). Efficiency of focusing grating couplers versus taper length and angle. *Journal of Physics: Conference Series,* 1410 012181.

Nambiar, S., Kallega, R. and Selvaraja, S. K. (2019). High-efficiency Grating Coupler in 400 nm and 500 nm PECVD Silicon Nitride With Bottom Reflector. *EEE Photon. Jour.,* PP(99):1-1.

O'Brien, J. L., Furusawa, A. and Vuckovic, J. (2009). Photonic quantum technologies. *Nat. Photon.*, 3:687–695.

Song, J. H., Kongnyuy, T. D., Troia, B., Saseendran, S. S., Soussan, P., Jansen, R. and Rottenberg X. (2019). Grating devices on a silicon nitride technology platform for visible light applications. *OSA Continuum Vol*. 2, No. 4:1155-1165.

Wang, L., Wang, Y. and Zhang X. (2012). Embedded metallic focus grating for silicon nitride waveguide with enhanced coupling and directive radiation. *Opt. Exp.*, No. 16, Vol. 20.